Chapter 1
Self-Organization of Pristine C_{60} Fullerene and its Complexes with Chemotherapy Drugs in Aqueous Solution as Promising Anticancer Agents

Leonid A. Bulavin, Yuriy Prylutskyy, Olena Kyzyma, Maxim Evstigneev, Uwe Ritter and Peter Scharff

Abstract The self-organization of pristine C_{60} fullerene and its complexation with chemotherapy drugs (in particular, doxorubicin, cisplatin and landomycin A) in aqueous solution were reviewed as a possible key stage of the mechanism of the in vivo and in vitro biological synergy, observed when these drugs are administered along with C_{60} fullerene. The results of application of various physico-chemical methods have been analyzed enabling to get insight into the nature of forces

L. A. Bulavin · O. Kyzyma
Faculty of Physics, Taras Shevchenko National University of Kyiv, Volodymyrska Str., 64, Kyiv 01601, Ukraine
e-mail: bulavin221@gmail.com

O. Kyzyma
e-mail: alyona_kizima@mail.ru

Y. Prylutskyy (✉)
ESC "Institute of Biology and Medicine", Department of Biophysics and Medical Informatics, Taras Shevchenko National University of Kyiv, Volodymyrska Str., 64, Kyiv 01601, Ukraine
e-mail: prylut@ukr.net

O. Kyzyma
Joint Institute for Nuclear Research, 6 Joliot-Curie Str., 141980 Dubna, Moscow reg., Russia

M. Evstigneev
Belgorod State University, 85 Pobedy Str., 308015 Belgorod, Russia
e-mail: max_evstigneev@mail.ru

U. Ritter · P. Scharff
Institute of Chemistry and Biotechnology, Technical University of Ilmenau, 25 Weimarer Str., 98693 Ilmenau, Germany
e-mail: uwe.ritter@tu-ilmenau.de

P. Scharff
e-mail: peter.scharff@tu-ilmenau.de

L. A. Bulavin and A. V. Chalyi (eds.), *Modern Problems of Molecular Physics*, Springer Proceedings in Physics 197, https://doi.org/10.1007/978-3-319-61109-9_1

stabilizing complexes of C_{60} fullerene with these drugs. A physico-chemical mechanism has been proposed allowing, at least in part, to explain the C_{60}-drug biological interaction.

1.1 Introduction

C_{60} fullerenes have been intensively investigated in the last decades mainly because of the vast range of their potential applications in biomedicine [1, 2]. Due to its nanometer size the pristine C_{60} fullerenes are able to interact with biomolecules and penetrate through the cell membrane [3–5]. They exhibit antioxidant properties and, being non-toxic (at low concentration at least) [6–10], exert specific health effects (e.g. suppress the growth of malignant tumors [11, 12]) and display biological synergy with antitumor drugs [13–15]. Although these molecules have extremely low water solubility, they form stable colloid solutions containing individual C_{60} fullerenes as well as C_{60} fullerene aggregates (clusters) in water, when subjected to extended mixing, sonication or solvent exchange [16, 17]. To understand behavior of C_{60} fullerene in the biological medium (at the levels of cell, tissue and organ) and its interaction with drugs, it is necessary to know exactly its concentration in water (dose effect), distribution in size and shape (size effect). Because the biomedical effects of the C_{60} fullerene nanoparticles directly depend on these properties [18, 19], their knowledge will enable understanding of 'which form of C_{60} fullerene is bioactive, namely a single molecule or its cluster?' and 'how this molecule interact with other drugs in biological media?'

In this chapter we shall briefly review the recent advances in physico-chemical characterization of pristine C_{60} fullerene and its interaction with antitumor drugs in aqueous solutions.

1.2 Self-Organization of C_{60} Fullerene Particles in Aqueous Solution

Investigations of the behavior of pristine C_{60} fullerene particles in aqueous solution have been undertaking since the end of 90-ies when the method of preparation of stable water colloid solutions had become routinely available [17, 20, 21]. By that time much had already been known on the properties of C_{60} fullerene in organic solvents, which had, in part, facilitated analogous studies in aqueous solutions.

To date, the C_{60} fullerene is considered as a colloidal particle due to the fact that its diameter equals to 10 Å. This conclusion originates from traditional point of view that the 10 Å border corresponds to the lower border of the colloidal range of dispersity, and the range of true solutions is under this limit [22]. Thus, aqueous solutions of any C_{60} fullerenes must feature properties of colloidal systems,

which contain associates of solvated C_{60} fullerenes of different size. Theoretical analysis of possible hydrated $(C_{60})_N$ clusters had shown, that the smallest stable C_{60} fullerene cluster (I_h symmetry group) consists of 13 C_{60} molecules [23, 24]. Its diameter is 3.36 nm (accounting for a molecular diameter of the water molecule), which is in excellent agreement with the scanning tunneling microscopy data [25]. More extended analysis revealed that cluster diameters regularly rise within the range from 3.4 to 36 nm, viz. 3.4, 7.1, 10.9, 14.5, 18.1, 21.8, 25.4, 28.8, 32.4, and 36.0 nm [25], i.e. each following particle is larger than the preceding one by 3.4–3.8 nm. Hence, it is considered that this row of C_{60} fullerene nanoparticles should be formed of hydrated $(C_{60})_{13}$ clusters. Thus, further investigation of the C_{60} fullerene aqueous solution (C_{60}FAS) had been split on characterization of the clusters' structure and morphology, and understanding the mechanism of cluster formation.

1.2.1 Characterization of the C_{60} Fullerene Aqueous Solution

A variety of physico-chemical methods has been applied in order to understand the specificity of C_{60} fullerene cluster formation. Characterization of C_{60} fullerene particles in aqueous solutions has been accomplished by means of UV-Vis spectroscopy [23, 24, 26–29], electron and tunneling microscopy [26, 30–35], atomic-force microscopy (AFM) [26, 36], zeta-potential [26, 32, 37, 38], dynamic light scattering (DLS) [26, 30, 32–34, 39], FTIR/Raman spectroscopy [27–29, 35, 36], small angle neutron scattering (SANS) [16, 29, 36, 40] and some other methods.

The most direct and readily accessible UV-Vis spectroscopy evidenced the existence of three most intense broad UV absorption bands with maxima at 208, 265 and 347 nm and generally resembles that in organic solvents (Fig. 1.1a) [26, 27]. The assignment of these bands to particular electron transitions, and the computation of the corresponding electronic parameters have been done [23]. The common feature of the UV-Vis spectra of C_{60}FAS is the light scattering, most evidently seen on dilution and affecting the value of the absorption.

The composition of C_{60}FAS was typically monitored using AFM and tunneling/electron microscopy techniques [26, 30–36]. The typical AFM picture is given in Fig. 1.1c; the similar pictures have been reported during the past 10 years by different research groups. The picture demonstrates randomly arranged individual C_{60} molecules with diameter ~0.7 nm and their bulk sphere-like aggregates with a height of 2–50 nm. Interestingly, some individual C_{60} fullerene aggregates with a height of ~100 nm were also reported in the probe microscopy images, indicating a polydisperse nature of C_{60}FAS, including either monomers or aggregates having diameters ranging from several to hundreds of nanometers.

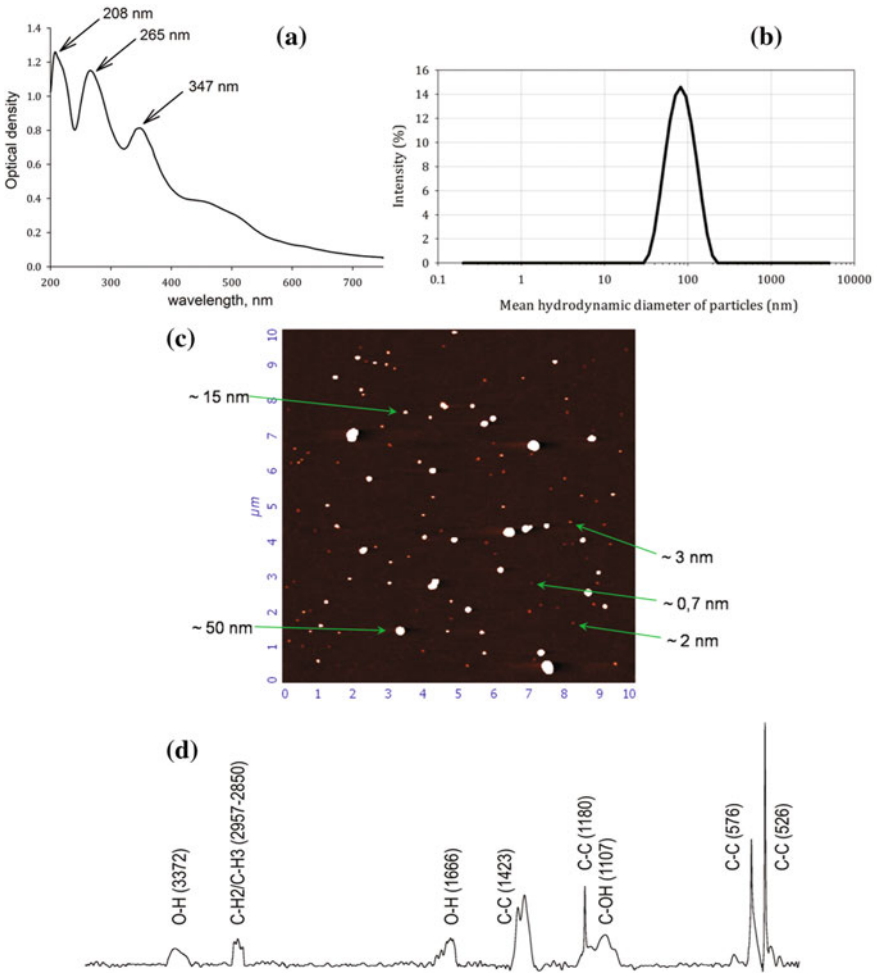

Fig. 1.1 Examples of experimental data measured for C_{60}FAS: UV-Vis spectrum (**a**), DLS spectrum (**b**), AFM image (**c**), IR spectrum (**d**). Redrawn from [26, 36, 54]

The results from microscopy images have also been confirmed by DLS and SANS data [16, 26, 29, 30, 32–34, 36, 39, 40]. The wide distribution of hydrodynamic dimensions of C_{60} fullerene particles by intensity with *z*-average ~70–120 nm (Fig. 1.1b) most directly evidences the polydispersity, independently supported by SANS. The gyration radii $R_g = 15…20$ nm calculated from the latter method well agrees with the dimensions of the particles seen in AFM. Importantly, the existence of 'slow' aggregation (in the scale of months) of C_{60} fullerenes, resulting in increase of R_g was reported in aqueous solution similar to

that established before in organic solvents [32, 33, 39, 41]. However, no significant alteration of the aggregate structures and properties of polydispersity were noted. Moreover, experimental data indicate that the structural and morphological features of polydisperse C_{60} fullerene aggregates present in aqueous solution remain essentially similar for different methods of C_{60}FAS preparation as well [36].

The magnitude of the zeta-potential, which is related to the stability of colloid dispersions, spans in relatively wide range from −9 mV up to −38 mV [21, 26, 37, 38] and evidences the presence of negative charge on the surface of C_{60} molecule in solution. A high negative charge of colloid clusters (or, more strictly, the electrostatic repulsion between the negatively charged clusters) plays significant role in the stabilization of C_{60}FAS (i.e. it disfavors the aggregation and makes the solution electrically stable).

The presence of negative charge on C_{60} fullerene surface is a generally accepted fact and is considered to be the key, but not the sole factor of C_{60} fullerene solubility in aqueous solution. The formation of the ordered, H-bonded and sphere-like hydrated shells around fullerene's surface, is another important issue extensively discussed over the past decade [27, 29, 30, 35, 36, 42–46]. However, recent FTIR spectroscopy data suggested that there is one more factor which should also be considered [35, 36]. The FTIR spectrum of C_{60}FAS (Fig. 1.1d) displays the typical pattern of peaks which could be expectedly assigned to C-C vibrational modes of C_{60} molecule. However, additional peaks were reported independent of the method of C_{60}FAS preparation and corresponded to C-O stretching. It strongly suggests that C_{60} fullerene cage is hydroxylated and hydroxyls forming alcohol functional groups exist in the structure of C_{60} fullerene in water. Hence the primary mechanism of C_{60} fullerene solubilization in water could be the attachment of the OH-groups to C_{60} fullerene carbons [35, 36] which explains why the lone C_{60} molecules and their clusters exist at equilibrium in solution for quite a long time. It also explains the irreversible character of the adsorption/desorption isotherms [30], the minimal extraction of C_{60} fullerene from water-colloid solutions by toluene [21], and the ability of C_{60} fullerenes from aqueous solution to hold water molecules even in vacuum [27]. The covalent attachment of the OH-groups does not exclude the possibility of electron transfer from water molecules to C_{60} fullerene enabling to explain the negative charge of C_{60} fullerene particles. It follows that the previous model of stabilization of hydrated C_{60} fullerene by water molecules joined together by H-bonding network [27, 29] needs to be revisited with mandatory account for the available results of molecular dynamics simulations of hydrated C_{60} fullerenes [43–46]. The latter reports weakening and breakage of the H-bonds between water molecules in immediate vicinity of the C_{60} fullerene surface and the overall dynamic character of the hydration shell around C_{60} fullerene particles in water.

1.2.2 Aggregation of the C_{60} Fullerenes in Aqueous Solution

So far the effect of cluster formation (or aggregation) has been extensively studied in terms of the kinetics of aggregation and the equilibrium distribution of C_{60} fullerene clusters [7, 16, 17, 21, 23–36, 39–41]. It has been recently established that the aggregates of pristine C_{60} fullerenes provide an excellent template for formation of highly ordered inclusion complexes with other molecules, resulting in amplified physico-chemical or biological properties [47, 48]. Apart from the basic physico-chemical interest to the aggregation process, it was recently found that the in vitro toxicity of C_{60} fullerene is correlated with its ability to undergo aggregation [49] and specifically the aggregated forms of C_{60} fullerene may effectively bind with biopolymers [50]. Therefore the C_{60} fullerene aggregation is considered now to be of general interest.

It has long been noted that under the dilution and simultaneous light mechanical shaking of C_{60}FAS, the large clusters can dissociate into the small ones, similar to that observed before in C_{60} fullerene benzene solution. It has also been established that the C_{60} fullerene solutions undergo 'fast' and 'slow' kinetics of cluster formation [23, 32, 33, 41]. The former is considered to be diffusion-limited and the latter is reaction-limited. Under first approximation the 'fast' mode occurs at typical diffusion timescale and thereby resembles equilibrium aggregation process well known for small molecules in solution [51]. It still remains relatively poorly investigated. The 'slow' mode occurs in the timescale of days and months, and has been extensively reviewed [41, 52]. Below we shall focus on thermodynamics of the equilibrium aggregation of C_{60} fullerene nanoparticles.

Surprisingly, determination of thermodynamical parameters of aggregation, such as equilibrium aggregation constant, or enthalpy/entropy/Gibbs free energy changes have been accomplished in just a few works [43, 44, 53–55]. Possible reasons for this include an incomplete understanding of the microscopic picture of C_{60} fullerene cluster formation in solution, and, as a consequence, difficulties in building a theoretical model of C_{60} fullerene aggregation. For example, a very complex interplay between the van der Waals, electrostatic and hydrophobic interactions on C_{60} fullerene aggregation, which presumably does not follow classical hydrophobic effect, was shown [42–44]. It points out that the overall thermodynamic picture of C_{60} fullerene aggregation in aqueous solution deviates from classical aggregation of small molecules, which makes this issue still a vacant niche for further research studies.

Presumably the first attempt to measure equilibrium C_{60} fullerene aggregation constant was accomplished in [54] by means of titrating the C_{60} fullerene aqueous solution and recording the intensity-averaged distributions of particles present in solution in DLS experiment. These data allow computing the mean hydrodynamic diameter, d_z (z-average), and translational diffusion coefficient, D, of light scattering particles. The corresponding experimental dependence of d_z on the C_{60} fullerene concentration, C_0 / r (where r is the dilution factor), is given in Fig. 1.2.

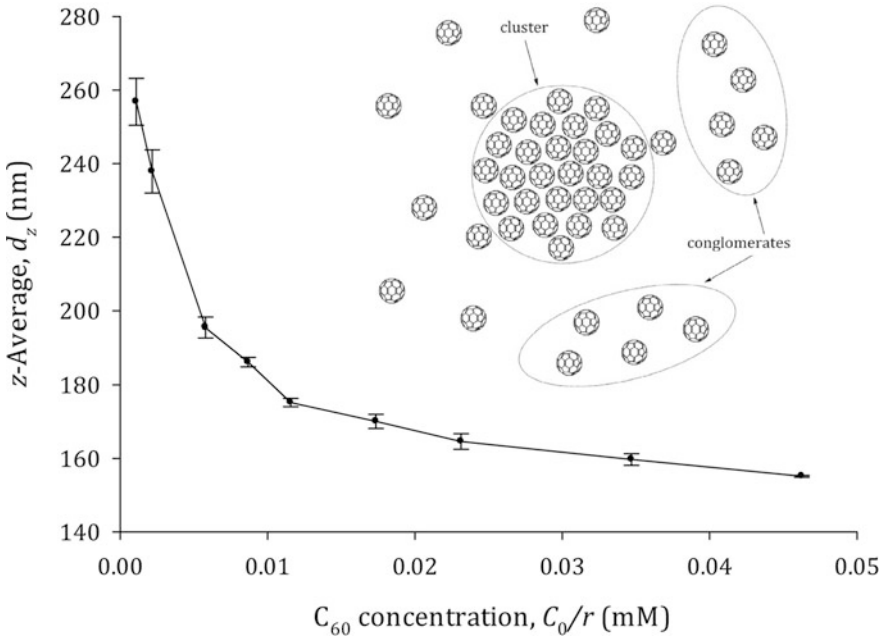

Fig. 1.2 Experimental dependence of z-average on C_{60} fullerene concentration. Redrawn from [54]

Currently the accepted position on the aggregation of small molecules in diluted aqueous solutions suggests that on increasing the concentration of the solute, the translational diffusion coefficient must decrease as a result of an increase in the aggregates' dimensions [56, 57]. Qualitatively, a similar view exists with respect to the aggregation of C_{60} fullerene as well, supported by theoretical computation of the dependence of D on C_{60} fullerene concentration in toluene [52]. However, the dependence $d_z(C_0/r)$ in Fig. 1.2 obtained using standard methods of C_{60}FAS preparation demonstrates the reverse behavior: increasing the solute concentration results in a decrease in the value of d_z. Unfortunately, direct comparison of these results with existing literature data is not possible, because these articles are restricted to dealing with measurements of D (or d_z) of C_{60} fullerene in solution at a single concentration point in each case (e.g. [32, 50]). However, analysis of literature data associated with small molecule aggregation suggests that on reaching micellar concentrations, the concentration dependence of the directly measured translational diffusion coefficient (e.g. by DLS or similar valid method) goes into reverse [58, 59]. This result is commonly interpreted in terms of the direct interaction of micelles with each other in solution due to non-covalent forces, an effect that has been known for some time [58, 59]. The micellar interaction acts as an addition to Brownian motion and, consequently, results in elevation of the diffusion coefficient on raising the solute concentration. Taking into account the polydisperse

nature of C_{60}FAS and the existence of C_{60} fullerene clusters with diameters in the magnitude range 10–100 nm, it was suggested that the reverse dependence of the $d_z(C_0/r)$ curve in Fig. 1.2 is a consequence of the interaction effect for $(C_{60})_n$ clusters [54]. Hence, the shape of the titration curve in Fig. 1.2 is governed by two opposite tendencies, viz. the aggregation leading to increase of d_z, and interaction of clusters leading to decrease of d_z.

Based on the DLS titration experiment a physical model of the C_{60} fullerene aggregation was suggested [54] (the so-called 'up-scaled model'). According to this model the aggregation occurs as a simultaneous binding of large number of small C_{60} fullerene particles or monomers (referred to as 'conglomerates', see Fig. 1.2) with large C_{60} fullerene clusters (nucleus of the cluster, considered not undergoing dissociation onto smaller ones). As a consequence of this process, the equilibrium distribution of C_{60} fullerene particles by dimension is formed, which can be quantified in terms of equilibrium aggregation constant K_F (or Gibbs free energy change, ΔG_F). The resultant equation enabling to calculate the experimental titration curve $d_z(C_0/r)$ in Fig. 1.2 is given as [54].

$$d_z = \frac{d_0}{1 + A' \frac{C'_{M0}}{r}} \cdot \frac{\left[1 + (B-1)BK_F C'_{R1}\right]^2 + B^3 K_F C'_{R1}}{\left(1 - BK_F C'_{R1}\right)^3 \sum_{i=0}^{\infty} (1+Bi)^{5/3} \left(BK_F C'_{R1}\right)^i}, \tag{1.1}$$

where

$$C'_{R1} = \frac{r + C'_{M0}BK_F + (C_0 - C'_{M0})K_F - \sqrt{\left(r + C'_{M0}BK_F + (C_0 - C'_{M0})K_F\right)^2 - 4rK_F(C_0 - C'_{M0})}}{2rBK_F},$$

C'_{M0}, A', K_F, B, d_0 are the search parameters, obtained by means of fitting the experimental curve in Fig. 1.2 with (1.1).

The reported value of the aggregation constant equals to $K_F = 56000\ \mathrm{M}^{-1}$ [54], well matching the theoretically calculated Gibbs free energy change in [53].

The titration experiment reviewed above and resulted in determination of K_F had been further complemented with estimation of enthalpy and entropy change associated with the aggregation process [55]. Direct calorimetric measurement of the heat effect on dilution and temperature dependence of z-average in DLS experiment had evidenced nearly zero enthalpy change. A final conclusion was made stating purely entropic character of the C_{60} fullerene aggregation. The main contribution to ΔG_F is considered to be due to hydrophobic interaction, i.e. liberation of water molecules weakly bound to C_{60} fullerene particles on cluster formation (i.e. those molecules belonging to distant hydration shells of the C_{60} fullerene particle). Importantly, in this process the first hydration shell surrounding C_{60} fullerenes remains essentially unchanged resulting in a contact distance between the surfaces of the interacting C_{60} fullerene particles larger than observed for typical aromatic-aromatic stacking (ca. 0.5 nm). Theoretical decomposition of ΔG_F onto

energetic contribution from various physical factors had shown that the net van der Waals and electrostatic terms appear to be relatively small due to the compensatory nature of the intermolecular interaction and the interaction with solvent on complex formation [54], additionally confirming the entropic nature of C_{60} fullerene aggregation in aqueous solution.

1.3 Self-Organization of C_{60} Fullerene-Antitumor Drug Mixtures

So far the possibility of modification of biological and/or physico-chemical properties of C_{60} fullerene or drug was mainly considered in terms of covalent conjugation of the drug molecules with C_{60} fullerene [47]. As a consequence, a series of C_{60}-drug conjugates were reported possessing improved properties [60, 61]. On the other hand, the presence in the structure of C_{60} molecule of aromatic surface composed of conjugated carbon rings suggests the possibility of its effective interactions via π-stacking with aromatic moieties of proteins, nucleic acid bases, aromatic vitamins, antibiotics and other compounds which may be present in a biosystem. Hence, the non-covalent complexation of C_{60} fullerenes with bio-receptors and aromatic drugs may contribute to some extent to the observed biological effects at the cellular and organism levels. Indirect justification of this hypothesis may come from the well-known fact that some cellular effects of the action of aromatic biologically active compounds may be interpreted in terms of their complexation in physiological medium [51]. During the past few years two sets of reports appeared evidencing a strong biological interaction in vitro and in vivo between C_{60} fullerene and the aromatic antitumor drugs, doxorubicin (Dox) [13–15, 62–64] and cisplatin (Cis) [65]. The peculiarity of this interaction was the following: (i) the most pronounced effect was observed during simultaneous administration of the drugs and C_{60} fullerene, (ii) the physico-chemical interaction of the drug with C_{60} fullerene is non-covalent, (iii) preliminary indices of the correlation of the in vitro biological effect with equilibrium constant of complexation of C_{60} fullerene with aromatic drug molecules were noted [64]. Thus the knowledge of how C_{60} molecules interact with aromatic drugs is important for understanding the mechanism of medico-biological action of C_{60} fullerenes.

Currently available data on the structure and thermodynamics of the interaction between C_{60} fullerenes and aromatic molecules are scarce and limited to systems mainly studied in non-polar solutions (see [66] and references therein) and several systems studied in aqueous solution [13, 62, 65–70]. Below we shall briefly review the main results of structural and thermodynamical analysis of the C_{60} fullerene interaction with Dox, Cis and novel angucycline antibiotic landomycin A (LA) [71] as the systems which have been most extensively investigated to date as compared to others.

1.3.1 C_{60} Fullerene Complexation with Doxorubicin

Antitumor antibiotic Dox belongs to the group of the most effective and extensively used drugs in chemotherapy of cancer. The principal limitation for its use is relatively high side toxicity, creating a long-standing challenge for generations of researchers attempting to minimize this drawback. As discussed above C_{60} fullerene was demonstrated to improve the medico-biological effect of Dox in vivo and in vitro making this drugs' combination of potential interest for clinical studies.

A range of various physico-chemical methods was applied in order to detect the complexation between C_{60} fullerene and antibiotic Dox [13, 62, 66, 68, 69]. In neutral solution conditions the Dox molecule bears positive charge, whereas the C_{60} fullerene is negatively charged.

The AFM investigation of the C_{60}-Dox mixture in low concentration range in non-salted aqueous solution evidenced the formation of new island-type structures (Fig. 1.3e), which were assigned to the complexes between the C_{60} and Dox molecules [68]. Similar situation was also reported in physiological solution, although in this case the interpretation of the results was strongly obscured by the presence of salt crystals [69]. The C_{60}-Dox interaction was also displayed by UV-Vis spectroscopy by hypochromic changes of the absorption maximum (Fig. 1.3a) with a slight bathochromic shift with increasing C_{60} fullerene concentration [13, 66, 68]. Quite expectedly the zeta-potential study of C_{60}-Dox mixture gave a pronounced positive shift of zeta-potential peak evidencing shielding of the C_{60} molecule negative charge and charging of these clusters by complexation of positively-charged Dox with C_{60} fullerene clusters [69]. The remarkable change in translational diffusional motion of Dox molecules on addition of C_{60} fullerene, monitored by diffusion-ordered NMR spectroscopy (DOSY), had also supported the existence of complexation (Fig. 1.3d) [68]. And, finally, the SANS data yielded the distribution function of pair distances, pointing out on the existence of at least two statistically different entities in solution, which are the C_{60} fullerene aggregates and the complexes between the C_{60} and Dox molecules (Fig. 1.3b) [62]. The qualitative experimental data were complemented by calculation of the most probable structure of the C_{60}-Dox complex, from which the maximal filling of the C_{60} fullerene surface by three Dox molecules was noted (Fig. 1.3c) [13, 66].

In contrast to the set of results reviewed above and concluded on the existence of complexation, an additional experimental dataset was reported, which had not directly supported this statement. First, at high C_{60} fullerene concentrations the UV-Vis hypochromic shift changes sign and becomes hypsochromic (Fig. 1.3a) [66]. The isothermal titration calorimetric measurements (ITC) had given nearly zero heat effect of C_{60} fullerene addition to Dox solution, and ^{1}H NMR titration curves had unexpectedly displayed very negligible changes inconsistent with the complexation hypothesis [68].

In addition, NMR DOSY titration curve for translational diffusion coefficient for Dox molecules exhibited reverse behavior (Fig. 1.3d) as compared to that initially

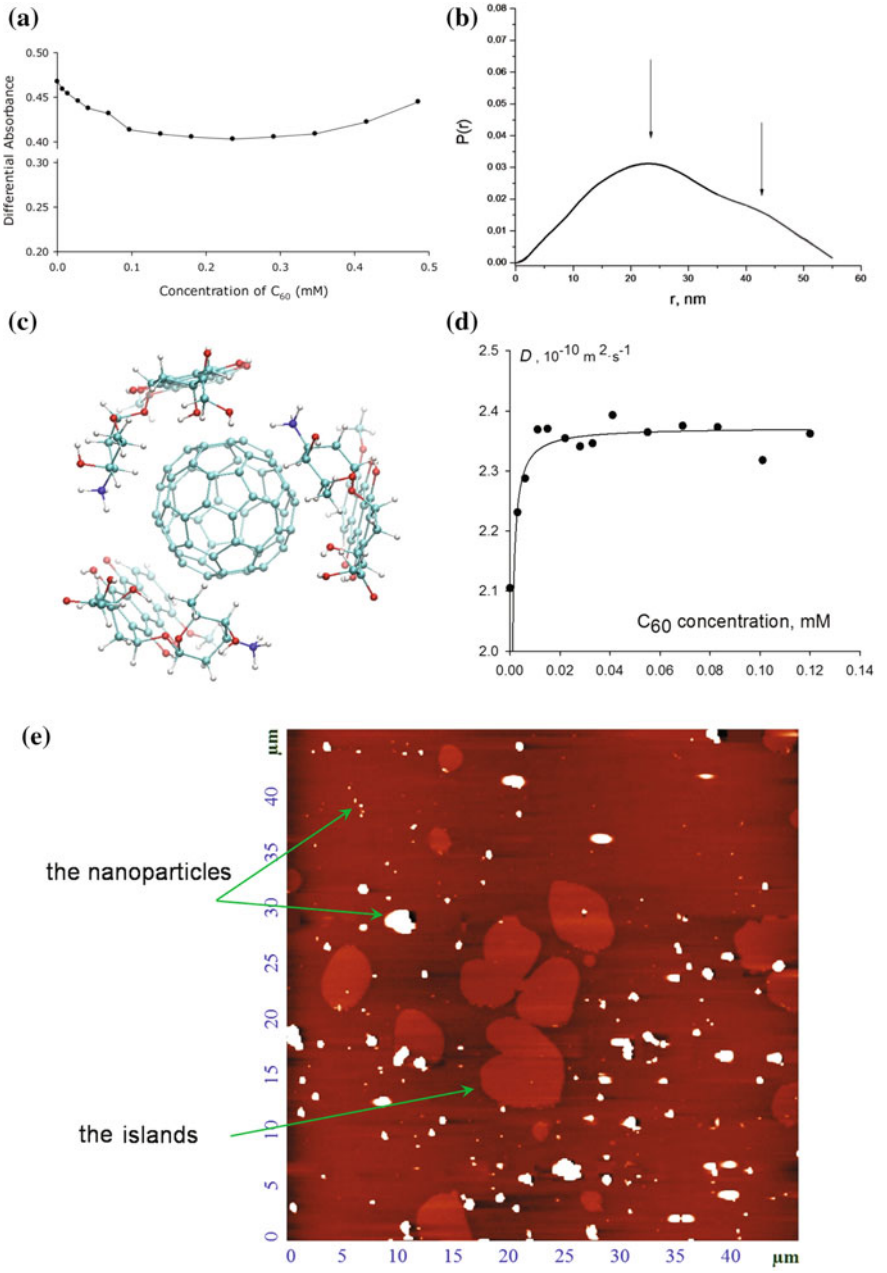

Fig. 1.3 Examples of experimental data measured for C_{60} fullerene-doxorubicin aqueous solution: UV-Vis titration curve (**a**), SANS pair distribution function (**b**), calculated C_{60}-Dox structure (**c**), DOSY translational diffusion coefficient (**d**), AFM image (**e**). Redrawn from [62, 66, 68]

expected (analogous to that discussed above for DLS titration experiment of C_{60} fullerene aqueous solution) [68].

The observed distinguishment of various physico-chemical methods, which directly evidence or demonstrate no signs of C_{60}-Dox complexation, received complete interpretation in [68]. The essence of this view is grounded on two main statements:

(i) the first hydration shell around the C_{60} fullerenes cannot be detached by Dox complexation, resulting in big distance (~0.5 Å) between the surfaces of Dox and C_{60} molecules in the complex. As a consequence, magnetic ^{1}H NMR shielding could be minimal (as evidenced in NMR experiment), and the enthalpic contribution from van der Waals and electrostatic forces could be damped (as evidenced in ITC experiment). Hence, the C_{60}-Dox complexation appears to be entropically-driven, i.e. mainly governed by hydrophobic force due to removal of water molecules from the second and higher-level hydration shells around C_{60} fullerene particles;

(ii) the binding of Dox molecules at moderate and high C_{60} fullerene concentrations mainly occurs by means of adsorption into large C_{60} fullerene clusters, resulting in the effect called 'ligand-induced C_{60} fullerene aggregation'. In brief, positively charged Dox molecules being absorbed by negatively-charged C_{60} fullerene clusters, induce additional cluster growth due to attenuated electrostatic repulsion between C_{60} molecules. It induces additional light scattering (as evidenced in UV-Vis experiment) and results in reverse self-diffusion behavior of Dox molecules (as evidenced in NMR DOSY experiment).

The physical model of C_{60}-Dox interaction outlined in these two statements enabled to build the thermodynamical model of their interaction and compute the corresponding equilibrium hetero-complexation constant, $K_L \approx 6000\ \mathrm{M}^{-1}$ [66]. This value was further used to correlate the relative in vitro biological effect of the action of C_{60}-Dox mixture on human buccal epithelium cells [64] and to compare the C_{60} fullerene hetero-complexation affinity to various drugs [66].

1.3.2 C_{60} Fullerene Complexation with Cisplatin

Aqueous soluble inorganic derivative of bi-valent platinum, i.e. cisplatin (Cis-[Pt(II)$(NH_3)_2Cl_2$]), is currently one of most extensively used chemotherapeutic drug for cancer treatment. Similar to Dox, the principal drawback of Cis is its side toxicity limiting its use in clinical practice. However, the success in improving the medico-biological effect of Dox by mixing it with C_{60} fullerene (see above) had inspired similar studies with C_{60}-Cis mixture, yielding positive outcome in vivo and in vitro [65].

Investigation of possible complexation between C_{60} fullerene and Cis has been carried out using generally similar protocol as that reviewed above for C_{60}-Dox interaction [70]. It should be noted that the direct complexation between C_{60} and Cis molecules should likely be relatively weak as compared with C_{60}-Dox system, because the π-stacking in the former case would be absent. Quite expectedly, the UV-Vis spectra (Fig. 1.4b) gave minor signs of interaction, and ITC demonstrated nearly zero heat effect. In contrast, SANS-derived pair distribution function (Fig. 1.4c) had evidenced the existence of two apparent statistically different entities in aqueous solution, one of which was assigned to the C_{60}-Cis complexes. This finding was partly supported by SEM and DLS studies (Fig. 1.4a, d). The latter investigation demonstrated apparent shift of the distribution of hydrodynamic radii of light scattering particles to higher numbers on addition of Cis to C_{60} fullerene aqueous solution. The ab initio structure of the C_{60}-Cis complex was shown to feature stable energy minimum.

In general, the revealed patterns of physico-chemical interaction of C_{60} fullerene with Cis have been found to resemble much the interaction of C_{60} molecule with antitumor antibiotic Dox, reviewed above. The complexation of Cis with C_{60} fullerene is entropic by origin and is totally driven by hydrophobic interactions. The binding of Cis occurs mainly into large C_{60} fullerene clusters via non-specific adsorption, although the existence of weak 1:1 C_{60}-Cis complexes could not be ruled out.

1.3.3 C_{60} Fullerene Complexation with Landomycin A

LA is a new antitumor antibiotic of angucycline group, possessing high antitumor activity against cancer cells of different origin, which induces early apoptosis in target cells [72–76].

The AFM image displaying the content of aqueous mixture of C_{60} fullerene with LA is given in Fig. 1.5a. The observed aggregates having the height of 2–25 nm may either be related to C_{60} fullerene and LA. The point nano-objects with the height of 0.6–1.8 nm may also be associated with C_{60} fullerene or LA molecules, or their complexes, which seem to be undistinguishable due to similarity of the LA and C_{60} fullerene dimensions.

In contrast to AFM results, the DLS data evidence apparent shift of the z-average on addition of LA to C_{60}FAS (Fig. 1.5b). However, the most interesting is the concomitant change in the shape of distribution of light scattering particles, which becomes narrower and shifts to larger dimensions. This observation means that LA solution affects the distribution of C_{60} fullerene clusters and indirectly points out on the possibility of interaction between the LA and C_{60} molecules. The magnitude of zeta-potential measured for C_{60}-LA mixture had shifted up to −10 mV from the initial value of −22.1 mV measured for C_{60}FAS additionally confirming the possibility of interaction. And, finally, the SANS experiment had also evidenced the changes in scattering signal in the C_{60}-LA mixture. As seen from Fig. 1.5c in small

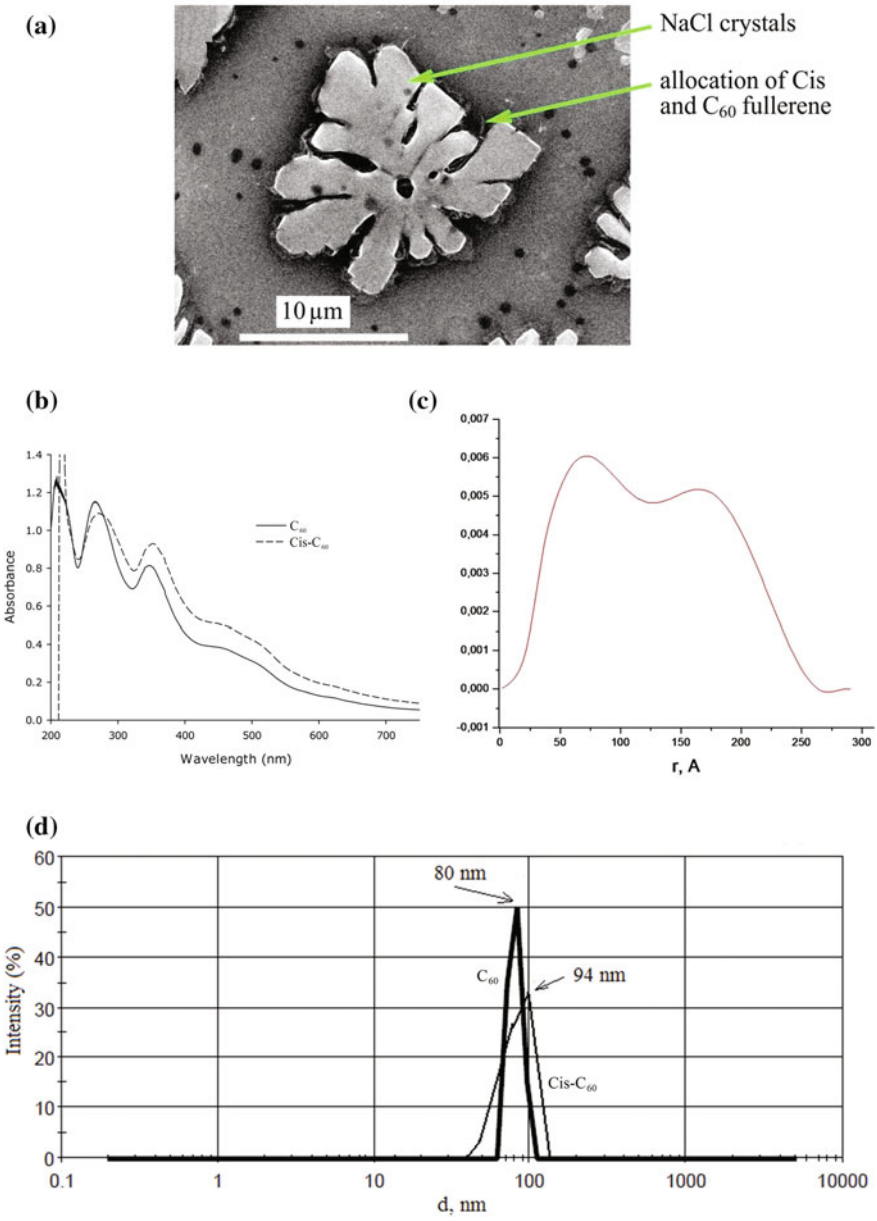

Fig. 1.4 Examples of experimental data measured for C_{60} fullerene-cisplatin aqueous solution: SEM image (**a**), UV-Vis spectrum (**b**), SANS pair distribution function (**c**), DLS spectrum (**d**). Redrawn from [70]

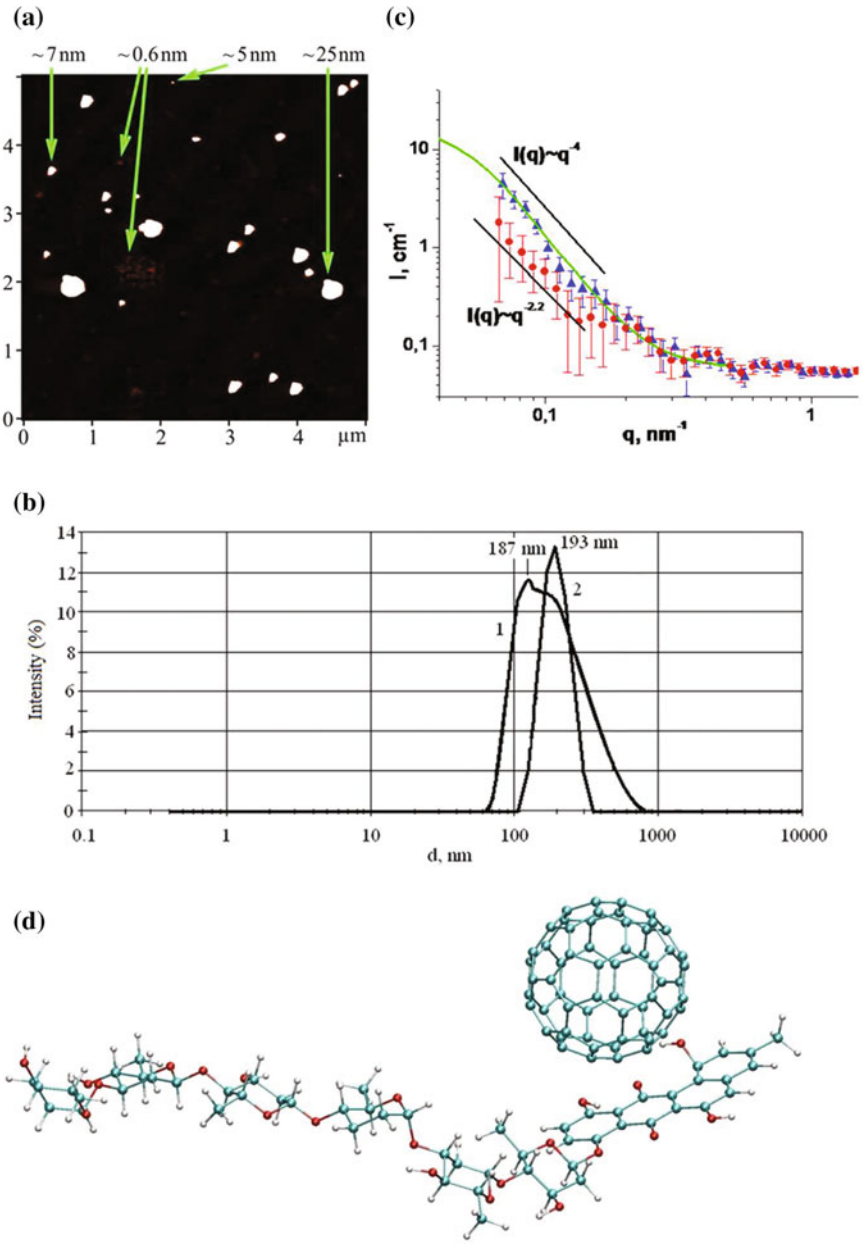

Fig. 1.5 Examples of experimental data measured for C_{60} fullerene-landomycin A aqueous solution: AFM image (**a**), DLS spectrum (**b**), SANS data (C_{60}FAS—triangle, C_{60}-LA mixture—circle) (**c**), calculated C_{60}-LA structure (**d**). Redrawn from [79]

q-region the behavior of scattering intensity changes from $I(q) \sim q^{-4}$ for C_{60}FAS to $I(q) \sim q^{-2.2}$ for the mixture with LA. Such alteration of the scattering curve suggests that compact spherical C_{60} fullerene clusters in aqueous solution are changed to fractal-type organization of the aggregates with mass fractal dimension, $D = 2.2$, in the C_{60} fullerene mixture with drug.

LA is an aromatic compound containing flat benz[a]anthraquinone chromophore. As a consequence the most probable arrangement of the molecules in 1:1 C_{60}-LA complex is the π-stacked structure outlined in Fig. 1.5d. The principal contribution to the stability of such complex is given by the interactions between the drug's chromophore and C_{60} fullerene surface, and the role of deoxyoligosaccharide chain seems to be minor.

1.4 Conclusions

The self-organization of C_{60} fullerene and its complexation with chemotherapy drugs (in particular, doxorubicin (Dox), cisplatin (Cis) and landomycin A (LA)) in aqueous solution were reviewed in this chapter as a possible key stage of the mechanism of the in vivo and in vitro biological synergy, observed when these drugs are administered along with C_{60} fullerene. Although the investigated drugs are very different in terms of chemical structure and properties, their thermodynamic patters of binding with C_{60} fullerene were found to be generally similar. Apart from certain specificities of binding, the complexation was found generally non-specific, entropic by origin and occurring mainly into large C_{60} fullerene clusters, governed by hydrophobic interactions. This physico-chemical mechanism may be further transferred onto biological system, viz. on simultaneous administration the hydrophobic C_{60} fullerene clusters incorporating Cis, Dox or LA molecules protect them from reactive environment when moving in biological fluid. Hence, these clusters may act as a delivery system and elevate the active concentration of the drug which induces biological effect. Such mechanism, at least in part, explains the biological synergy observed experimentally for C_{60}-Cis and C_{60}-Dox mixtures. Apparently, this is a speculative model which requires further investigation and may just be used as a starting hypothesis in further studies of C_{60}-drug biological interactions. On the other hand, the use of C_{60} fullerene as a potential delivery system is extensively discussed now in scientific literature (see for review [47]). The model thus suggested agrees well with the mechanism of entrapment of surface active compounds by C_{60} fullerene clusters [77], and may probably shed light on the mechanism of biological synergy observed on simultaneous administration of fullerenol with Dox [78], which has not received explanation so far.

Acknowledgements This work was, in part, supported by Russian Science Fund (project no. 14-14-00328) and STCU project N6256.

References

1. F. Cataldo, T. Da Ros (eds.), *Medicinal Chemistry and Pharmacological Potential of Fullerenes and Carbon Nanotubes. Series: Carbon Materials: Chemistry and Physics* (Springer, Netherlands, 2008)
2. P. Anilkumar, F. Lu, L. Cao et al., Fullerenes for applications in biology and medicine. Current Med. Chem. **18**, 2045 (2011)
3. V.V. Turov, V.F. Chehun, T.V. Krupskaya et al., Effect of small addition of C_{60} fullerenes on the hydrated properties of nanocomposites based on highly dispersed silica and DNA. Chem. Phys. Lett. **496**, 152 (2010)
4. S. Foley, C. Crowley, M. Smaihi et al., Cellular localisation of a water-soluble fullerene derivative. Biochem. Biophys. Res. Commun. **294**, 116 (2002)
5. S. Prylutska, R. Bilyy, M. Overchuk et al., Water-soluble pristine fullerenes C_{60} increase the specific conductivity and capacity of lipid model membrane and form the channels in cellular plasma membrane. J. Biomed. Nanotechnol. **8**, 522 (2012)
6. S.V. Prylutska, I.I. Grynyuk, O.P. Matyshevska et al., Anti-oxidant properties of C_{60} fullerenes in vitro. Fuller. Nanotub. Carbon Nanostruct. **16**, 698 (2008)
7. G. Andrievsky, V. Klochkov, L. Derevyanchenko, Is the C_{60} fullerene molecule toxic?! Fuller. Nanotub. Carbon Nanostruct. **13**, 363 (2005)
8. N. Levi, R. Hantgan, M. Lively et al., C_{60}-Fullerenes: detection of intracellular photoluminescence and lack of cytotoxic effects. J. Nanobiotechnol. **4**, 14 (2006)
9. S.V. Prylutska, O.P. Matyshevska, A.A. Golub et al., Study of C_{60} fullerenes and C_{60}-containing composites cytotoxicity in vitro. Mater. Sci. Eng. C **27**, 1121 (2007)
10. J. Kolosnjaj, H. Szwarc, F. Moussa, Toxicity studies of fullerenes and derivatives. Adv. Exp. Med. Biol. **620**, 168 (2007)
11. H.J. Johnston, G.R. Hutchison, F.M. Christensen et al., The biological mechanisms and physicochemical characteristics responsible for driving fullerene toxicity. Toxicol. Sci. **114**, 162 (2010)
12. S.V. Prylutska, A.P. Burlaka, Y.I. Prylutskyy et al., Pristine C_{60} fullerenes inhibit the rate of tumor growth and metastasis. Exp. Oncol. **33**, 162 (2011)
13. S.V. Prylutska, A.P. Burlaka, P.P. Klymenko et al., Using water-soluble C_{60} fullerenes in anticancer therapy. Cancer Nanotechnol. **2**, 105 (2011)
14. R.R. Panchuk, S.V. Prylutska, V.V. Chumak et al., Application of C_{60} fullerene-doxorubicin complex for tumor cell treatment *in vitro* and in vivo. J. Biomed. Nanotechnol. **11**, 1139 (2015)
15. S. Prylutska, L. Skivka, G. Didenko et al., Complex of C_{60} fullerene with doxorubicin as a promising agent in antitumor therapy. Nanoscale Res. Lett. **10**, 499 (2015)
16. S.V. Prylutska, V.F. Korolovych, Y.I. Prylutskyy et al., Tumor-inhibitory effect of C_{60} fullerene complex with doxorubicin. Nanomed. Nanobiol. **2**, 49 (2015)
17. M.V. Avdeev, A.A. Khokhryakov, T.V. Tropin et al., Structural features of molecular-colloidal solutions of C_{60} fullerenes in water by small-angle neutron scattering. Langmuir **20**, 4363 (2004)
18. N.O. Mchedlov-Petrossyan, Fullerenes in liquid media: an unsettling intrusion into the solution chemistry. Chem. Rev. **113**, 5149 (2013)
19. Yu. Rud, L. Buchatskyy, Y. Prylutskyy et al., Using C_{60} fullerenes for photodynamic inactivation of mosquito iridescent viruses. J. Enzym. Inhib. Med. Chem. **27**, 614 (2012)
20. Z. Chen, R. Mao, Y. Liu, Fullerenes for cancer diagnosis and therapy: preparation, biological and clinical perspectives. Curr. Drug Metab. **13**, 1035 (2012)
21. G.V. Andrievsky, M.V. Kosevich, O.H. Vovk et al., On the production of an aqueous colloidal solution of fullerenes. J. Chem. Soc., Chem. Commun. **12**, 1281 (1995)
22. S. Deguchi, R.G. Alargova, K. Tsujii, Stable dispersions of fullerenes, C_{60} and C_{70}, in water. Prep. Charact. Langmuir **17**, 6013 (2001)

23. H.R. Kruyt (ed.), Colloid Science. vol. 1 Non-reversible systems (Moscow, Russia, 1955), 538p. (Russ. Transl.)
24. Y.I. Prylutskyy, S.S. Durov, L.A. Bulavin et al., Structure and thermophysical properties of fullerene C_{60} aqueous solutions. Int. J. Thermophys. **22**, 943 (2001)
25. L. Bulavin, I. Adamenko, Y. Prylutskyy et al., Structure of fullerene C_{60} in aqueous solution. Phys. Chem. Chem. Phys. **2**, 1627 (2000)
26. G.V. Andrievsky, V.K. Klochkov, E.L. Karyakina et al., Studies of aqueous colloidal solutions of fullerene C_{60} by electron microscopy. Chem. Phys. Lett. **300**, 392 (1999)
27. U. Ritter, Y.I. Prylutskyy, M.P. Evstigneev et al., Structural features of highly stable reproducible C_{60} fullerene aqueous colloid solution probed by various techniques. Fuller. Nanotub. Carbon Nanostruct. **23**, 530 (2015)
28. Z. Meng, S.M. Hashmi, M. Elimelech, Aggregation rate and fractal dimension of fullerene nanoparticles via simultaneous multiangle static and dynamic light scattering measurement. J. Colloid Interface Sci. **392**, 27 (2013)
29. A.O. Khokhryakov, M.V. Avdeev, V.L. Aksenov, L.A. Bulavin, Structural organization of colloidal solution of fullerene C_{60} in water by data of small angle neutron scattering. J. Mol. Liq. **127**, 73 (2006)
30. Y.I. Prylutskyy, V.I. Petrenko, O.I. Ivankov et al., On the origin of C_{60} fullerene solubility in aqueous solution. Langmuir **30**, 39–67 (2014)
31. J. Labille, J. Brant, F. Villieras et al., Affinity of C_{60} fullerenes with water. Fuller. Nanotub. Carbon Nanostruct. **14**, 307 (2006)
32. K.L. Chen, M. Elimelech, Relating colloidal stability of fullerene (C_{60}) nanoparticles to nanoparticle charge and electrokinetic properties. Environ. Sci. Technol. **43**, 7270 (2009)
33. J. Brant, H. Lecoanet, M.R. Wiesner, Aggregation and deposition characteristics of fullerene nanoparticles in aqueous systems. J. Nanopart. Res. **7**, 545 (2005)
34. K.L. Chen, M. Elimelech, Aggregation and deposition kinetics of fullerene (C_{60}) nanoparticles. Langmuir **22**, 10994 (2006)
35. J.A. Brant, J. Labille, J.Y. Bottero, M.R. Wiesner, Characterizing the impact of preparation method on fullerene cluster structure and chemistry. Langmuir **22**, 3878 (2006)
36. G.V. Andrievsky, V.K. Klochkov, A.B. Bordyuh, G.I. Dovbeshko, Comparative analysis of two aqueous-colloidal solutions of C_{60} fullerene with help of FTIR reflectance and UV-Vis spectroscopy. Chem. Phys. Lett. **364**, 8 (2002)
37. V.N. Bezmelnitsyn, A.V. Eletskii, M.V. Okun, E.V. Stepanov, Diffusion of aggregated fullerenes in solution. Phys. Scripta **53**, 364 (1996)
38. M. Wierzbicki, E. Sawosz, M. Grodzik et al., Comparison of anti-angiogenic properties of pristine carbon nanoparticles. Nanoscale Res. Lett. **8**, 195 (2013)
39. J. Labille, A. Masion, F. Ziarelli et al., Hydration and dispersion of C_{60} in aqueous systems: the nature of water-fullerene interactions. Langmuir **25**, 11232 (2009)
40. Y. Prilutski, S. Durov, L. Bulavin et al., Study of structure of colloidal particles of fullerenes in water solution. Mol. Cryst. Liq. Cryst. **324**, 65 (1998)
41. P. Scharff, K. Risch, L. Carta-Abelmann et al., Structure of C_{60} fullerene in water: spectroscopic data. Carbon **42**, 1203 (2004)
42. N.O. Mchedlov-Petrossyan, V.K. Klochkov, G.V. Andrievsky, Colloidal dispersions of fullerene C_{60} in water: some properties and regularities of coagulation by electrolytes. J. Chem. Soc., Faraday Trans. **93**, 4343 (1997)
43. J.H. Walther, R.L. Jaffe, E.M. Kotsalis et al., Hydrophobic hydration of C_{60} and carbon nanotubes in water. Carbon **42**, 1185 (2004)
44. L. Li, D. Bedrov, G. Smith, A molecular-dynamics simulation study of solvent-induced repulsion between C_{60} fullerenes in water. J. Chem. Phys. **123**, 204504 (2005)
45. L. Li, D. Bedrov, G.D. Smith, Water-induced interactions between carbon Nanoparticles. J. Phys. Chem. B **110**, 10509 (2006)
46. C.I. Wang, C.C. Hua, S.A. Chen, Dynamic solvation shell and solubility of C_{60} in organic solvents. J. Phys. Chem. B **118**, 9964 (2014)

47. J. Choi, S.D. Snow, J.-H. Kim, S.S. Jang, Interaction of C_{60} with water: first-principles modeling and environmental implications. Environ. Sci. Technol. **49**, 1529 (2015)
48. A. Montellano, T. Da Ros, A. Bianco, M. Prato, Fullerene C_{60} as a multifunctional system for drug and gene delivery. Nanoscale **3**, 4035 (2011)
49. Z.-Q. Li, Y.-M. Zhang, D.-S. Guo et al., Supramolecular assembly with multiple preorganised π-electronic. Cages Chem. Eur. J. **19**, 96 (2013)
50. D.Y. Lyon, L.K. Adams, J.C. Falkner, P.J. Alvarez, Antibacterial activity of fullerene water suspensions: effects of preparation method and particle size. J. Environ. Sci. Tech. **40**, 4360 (2006)
51. M. Song, S. Liu, J. Yin, H. Wang, Interaction of human serum album and C_{60} aggregates in solution. Int. J. Mol. Sci. **12**, 4964 (2011)
52. M.P. Evstigneev, Hetero-association of aromatic molecules in aqueous solution. Int. Rev. Phys. Chem. **33**, 229 (2014)
53. V.N. Bezmel'nitsyn, A.V. Eletskii, M.V. Okun, Fullerenes in solutions. Phys. Usp. **41**, 1091 (1998)
54. X. Zhao, A. Striolo, P.T. Cummings, C_{60} binds to and deforms nucleotides. Biophys. J. **89**, 3856 (2005)
55. Y.I. Prylutskyy, A.S. Buchelnikov, D.P. Voronin et al., C_{60} fullerene aggregation in aqueous solution. Phys. Chem. Chem. Phys. **15**, 9351 (2013)
56. D.P. Voronin, A.S. Buchelnikov, V.V. Kostjukov et al., Evidence of entropically driven C_{60} fullerene aggregation in aqueous solution. J. Chem. Phys. **140**, 104909 (2014)
57. D. Hazafy, M.-V. Salvia, A. Mills et al., NMR analysis of Nile Blue (C. I. Basic Blue 12) and Thionine (C. I. 52000) in solution. Dyes Pigment. **88**, 315 (2011)
58. A.A.H. Santiago, A.S. Buchelnikov, M.A. Rubinson et al., Shape-independent model (SHIM) approach for studying aggregation by NMR diffusometry. J. Chem. Phys. **142**, 104202 (2015)
59. M. Corti, V. Degiorgio, Quasi-elastic light scattering study of intermicellar interactions in aqueous sodium dodecyl sulfate solutions. J. Phys. Chem. **85**, 711 (1981)
60. D. Attwood, R. Blundell, V. Mosquera, Light scattering studies on the association of phenothiazine drugs in aqueous solutions of low ionic strength. J. Colloid Interface Sci. **157**, 50 (1993)
61. F. Lu, S.A. Haque, S.-T. Yang et al., Aqueous compatible fullerene—doxorubicin conjugates. J. Phys. Chem. C **113**, 17768 (2009)
62. J.-H. Liu, L. Cao, P.G. Luo et al., Fullerene-conjugated doxorubicin in cells. Appl. Mater. Interfaces **2**, 1384 (2010)
63. Y. Prylutskyy, A. Borowik, G. Gołuński et al., Biophysical characterization of the complexation of C_{60} fullerene with doxorubicin in a prokaryotic model. Mat-wiss u Werkstofftech **47**, 92 (2016)
64. S. Prylutska, I. Grynyuk, O. Matyshevska et al., C_{60} fullerene as synergistic agent in tumor-inhibitory doxorubicin treatment. Drugs R&D **14**, 333 (2014)
65. G.B. Skamrova, I.V. Laponogov, A.S. Buchelnikov et al., Interceptor effect of C_{60} fullerene on the in vitro action of aromatic drug molecules. Eur. Biophys. J. **43**, 265 (2014)
66. S. Prylutska, R. Panchuk, G. Gołuński et al., C_{60} fullerene enhances anticancer activity and overcomes tumor cells drug resistance. Nano Res. **10**, 652 (2017)
67. M.P. Evstigneev, A.S. Buchelnikov, D.P. Voronin et al., Complexation of C_{60} fullerene with aromatic drugs. Chem. Phys. Chem. **14**, 568 (2013)
68. A.S. Buchelnikov, V.V. Kostyukov, M.P. Yevstigneev, Y.I. Prylutskyy, Mechanism of complexation of the phenothiazine dye methylene blue with fullerene C_{60}. Russ. J. Phys. Chem. A **87**, 662 (2013)
69. Y.I. Prylutskyy, M.P. Evstigneev, I.S. Pashkova et al., Characterization of C_{60} fullerene complexation with antibiotic doxorubicin. Phys. Chem. Chem Phys. **16**, 23164 (2014)
70. Y.I. Prylutskyy, M.P. Evstigneev, V.V. Cherepanov et al., Structural organization of C_{60} fullerene, doxorubicin and their complex in physiological solution as promising antitumor agents. J. Nanopart. Res. **17**, 45 (2015)

71. Y.I. Prylutskyy, V.V. Cherepanov, M.P. Evstigneev et al., Structural self-organization of C_{60} and cisplatin in physiological solution. Phys. Chem. Chem. Phys. **17**, 26084 (2015)
72. J. Rohr, C. Hertweck, Comprehensive Natural Products II—Chemistry and Biology, eds. L. Mander, H.-W. Liu (Elsevier, Oxford, 2010), pp. 227–303
73. B. Ostash, A. Korynevska, R. Stoika, V. Fedorenko, Chemistry and biology of landomycins, an expanding family of polyketide natural products. Mini. Rev. Med. Chem. **9**, 1040 (2009)
74. M.K. Kharel, P. Pahari, M.D. Shepherd et al., Angucyclines: biosynthesis, mode-of-action, new natural products, and synthesis. Nat. Prod. Rep. **29**, 264 (2012)
75. L.V. Lehka, R.R. Panchuk, W. Berger et al., The role of reactive oxygen species in tumor cells apoptosis induced by Landomycin A. Ukr. Biochem. J. **87**, 72 (2015)
76. X. Yang, B. Fu, B. Yu, Total synthesis of Landomycin A, a potent antitumor angucycline antibiotic. J. Am. Chem. Soc. **133**, 12433 (2011)
77. M. Dalavalle, M. Leonzio, M. Calvaresi, F. Zerbetto, Explaining fullerene dispersion by using micellar solutions. Chem. Phys. Chem. **15**, 2998 (2014)
78. R. Injac, M. Perse, M. Cerne et al., Protective effects of fullerenol $C_{60}(OH)_{24}$ against doxorubicin-induced cardiotoxicity and hepatotoxicity in rats with colorectal cancer. Biomaterials **30**, 1184 (2009)
79. Y.I. Prylutskyy, V.V. Cherepanov, V.V. Kostjukov et al., Study of the complexation between Landomycin A and C_{60} fullerene in aqueous solution. RSC Adv. **6**, 81231 (2016)